11 January, 1998
Ed Lightbourn

Thermal Contact Conductance of Plastic/Aluminum Interface

ABSTRACT

Heated rollers are used in the forest product, printing and plastic processing industry to regulate product temperature during web processing. Improved temperature regulation results in a higher quality product as well as reduced waste and energy usage. A new experimental method to measure the joint contact conductance between the two surfaces of one rigid and one pliable material is developed and used to measure the thermal contact resistance of a different plastic sample to roller interfaces. Two blocks, initially at different temperatures, are brought together with the sample being studied between the blocks. The resulting time temperature profile can be used to determine the joint contact resistance. The physically static, thermally transient technique allows both joint resistance and thermal conductivity measurements to be made quickly and easily using minimal equipment. The average joint conductances measured for the polyester, polypropylene and embossed polyethylene samples were 1428 1250 and 345 W/m^2-K respectively over a pressure range of 0.25 to 7 kpa.

INTRODUCTION

Controlling the heat transfer from the roller to a web during processing is an important factor in obtaining a high quality finished product. The thermal joint conductance plays a large part in determining the heat transfer between the two surfaces, and is hard to predict analytically. Measurements of joint conductance for a pliable material in contact with a rigid surface have been accomplished in at least two ways. The contact conductance has been determined from dynamic measurements of a roller – web system (1), while other researchers have used a physically static, thermally steady-state technique (2-3).

As contact conductance is impossible to directly measure, it is inferred from temperature measurements. Accurate temperature measurements of thin plastic webs are difficult with non-contact temperature devices. Plastic radiation transmission spectrums vary widely according to the sample chemical composition, thickness, and the presence of any fillers, complicating the radiation sensor selection. Physically static, thermally steady-state methods often require both expensive equipment and a long time to run each test.

A new experimental technique based on physically static, thermally transient measurements circumvents the weaknesses of the two previous methods, and is especially suited to plastic samples. The method is easily adaptable to measuring the joint conductance of to the varying surfaces and conditions found in common plastics processing situations.

EXPERIMENTAL PROGRAM

An investigation of the joint conductance of various plastic films to a polished metal interface was undertaken to evaluate the methodology presented. The contact conductance was found as a function of both plastics type and interface pressure. The pressure range used in the study ranged from 0.3 to 7 kPa, commonly encountered in un-nipped heating cases. This is a lower pressure range then commonly studied.

The program is based on a method previously presented (4) to measure the thermal conductivity of coating materials. The solution is based on both an analytical and a finite difference solution to the transient response of a body undergoing a step response in the temperature boundary condition. In this method, two thermally lumpable bodies are placed in contact, with the plastic sample under consideration between the two blocks. The heat transfer between the two blocks is regulated by the total resistance between the two blocks. The total resistance between the two blocks was given as:

$$R''_{Total} = R''_{contact} + \frac{L_{sample}}{k_{sample}} + R''_{contact} \qquad (1)$$

Where $R^2_{contact}$ is the reciprocal of the joint conductance, $h^2_{contact}$. If either the joint conductance or the thermal conductivity of the sample was known, the other could be determined. In order to measure the thermal conductivity of a sample the sample would be coated with a thermally conductive grease to minimize the contact resistance. To measure the joint conductance, a sample of known conductivity was used in the tests, and the joint resistance was determined from eq. 1.

Apparatus Design and Setup

The apparatus schematic is shown in fig. 1; and consists of two aluminum blocks, surrounding insulation, data acquisition equipment, and a loading mechanism.

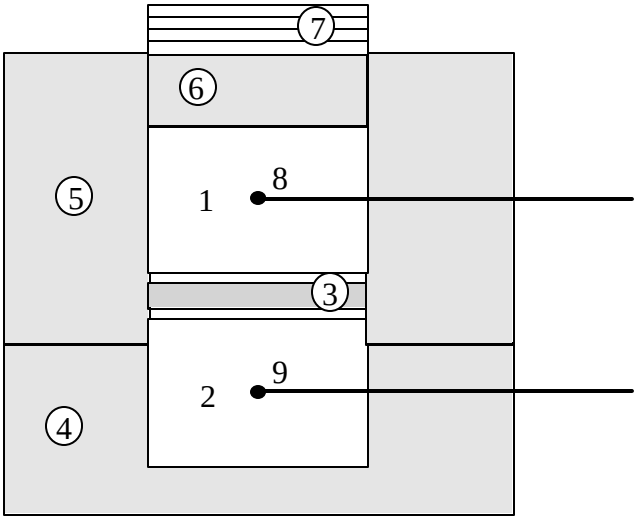

1	Top (Hot) Block	6	Load Insulation
2	Bottom (Cold) Block	7	Load (Variable)
3	Plastic Sample	8	Top Thermocouple
4	Bottom Insulation Cavity	9	Bottom Thermocouple
5	Top Insulation Cavity		

Fig. 1. Schematic of contact conductance measurement apparatus.

Two 2024 T4 Aluminum cylindrical blocks are used in the experiment. Both blocks were machined from a 7.62 cm diameter cylinder and each block was 5.08 cm high. One of the mating faces of each block was polished to a surface roughness Ra of 2.5 x 10^{-7} m.

Type T thermocouples were embedded along the axial center of the blocks with conductive silicone epoxy. An Omega Dyna-Res Data Acquisition System was used in this study to record the block, insulation and ambient temperature measurements. The thermocouples exhibited an accuracy of 0.7 °C relative to ambient. The hot block and cold block thermocouples matched within a maximum error of 0.3 °C over the range of the test conditions. Quick Log PC, also by Omega, was used as the data logging and control software. A 486 computer running Windows 95 was the host computer. Additional thermocouples were inserted in the insulation to determine the heat loss through the insulation through the environment. The signal conditioning board of the data acquisition system provided noise filtering and cold junction compensation for the thermocouples.

Expanded polystyrene insulation with a thermal conductivity of 0.048 W/m-K was used to surround the experimental system. The insulation was split into three pieces to allow the system to be assembled quickly and without supporting any of the load placed on the top block. This ensured that the interface pressure between the top and bottom block was equal to the sum of the top block and the external load all divided by the face area of the two blocks.

Before the start of each test the top block was heated to 60-70° K above ambient. The cold block, which was initially at room temperature, was placed in the bottom insulation cavity with a new plastic sample on top of the cold block. At the start of the test the data acquisition was begun. The hot block was then placed on top of the plastic sample, and the top insulation cavity was placed on top of the bottom insulation. Then the load insulation and the load were placed on top of the top block. Known masses were used as the load and varied to create different interface pressures.

Through the energy in the hot block is conducted through the plastic to the cold block and also conducted through the insulation to the surroundings. The cold block gained thermal energy from the hot block and lost energy by conduction through the insulation and to the surroundings. The total time for each test varied according the initial temperature difference between the two blocks and the joint resistance. The test duration ran from 4 minutes with the 0.02 mm polypropylene sample to 10 minutes with the 0.08 mm embossed polyethylene sample. The tests were stopped when the blocks came within 3° K of each other.

The solution to the transient temperature response for the two blocks was solved using two different methods. The first method used the lumped capacitance approach to model the two blocks. In the lumped capacitance approach, each block was assumed isothermal. The heat flows of each block were then modeled with a first order differential equation. As the blocks are placed in contact, the differential equations of the two blocks are coupled, and must be solved simultaneously.

The energy balance for a block can be represented by a model having the differential equation relating the energy increase (or decrease) of a block to the heat loss from the block to the surroundings and the energy transfer between the blocks. For each block the Energy balance related the energy inflows and outflows to the internal energy change of the blocks. For both blocks:

$$\dot{E}_{in} - \dot{E}_{out} = \frac{dE}{dt} \tag{2}$$

The energy out for both blocks was expressed as:

$$\dot{E}_{out} = h_{block} \cdot A_{surface} \cdot (T_{block} - T_{\infty}) \tag{3}$$

The hot block was considered block 1, and the cold block was block 2. For the hot block the energy transferred to the cold block was also a loss:

$$\dot{E}_{out} = \frac{A_{contact}}{R''_{total}} \cdot (T_1 - T_2) \tag{4}$$

The energy in for the cold block was:

$$\dot{E}_{in} = \frac{A_{contact}}{R''_{total}} \cdot (T_1 - T_2) \tag{5}$$

The mechanism equations were related to form the differential equations for each block. For block 1:

$$-c_p \cdot m_1 \cdot \frac{dT_1}{d\tau} = h_1 \cdot A_{surface} \cdot (T_1 - T_\infty) + \frac{A_{contact}}{R''_{Total}} \cdot (T_1 - T_2) \tag{6}$$

for block 2:

$$-c_p \cdot m_2 \cdot \frac{dT_2}{d\tau} = h_2 \cdot A_{surface} \cdot (T_2 - T_\infty) + \frac{A_{contact}}{R''_{Total}} \cdot (T_2 - T_1) \tag{7}$$

The differential equations were then solved analytically for to predict the hot and cold block temperatures over time.

The Biot number parameter is critical to the assumption of thermally lumped mass. The Biot number is defined in general as the ratio of the resistance to conduction heat transfer through the solid to the resistance to heat transfer from the solid to the surroundings. At ratios less than 0.1, the solid can be thermally lumped. For the experimental apparatus, the Biot parameter is the ratio between the resistance inside a block to the resistance to the heat flow between the blocks. For the two blocks and the contact resistance, the Biot number was equal to:

$$Bi = \frac{R''_{internal}}{R''_{external}} = \frac{L_{block}}{2 \cdot k_{aluminium} \cdot R''_{total}} \tag{8}$$

Where L_{block} is the height of each block. R''_{total} is as defined in eq. 1. For any run where the Biot number parameter was not less than 0.1, a lumped capacitance solution was inaccurate. As the Biot number was based on the total resistance between the two blocks, the conduction resistance of the plastic sample was important in the Biot parameter. For the thin (0.02 mm) polypropylene samples the Biot numbers approached 0.1, and a different approach had to be found for the data reduction.

The second solution method used a finite difference model of the blocks, plastic sample, and insulation system. As the finite difference program included an energy storage term for the energy balance on each node, the transient response of the two blocks could be predicted.

In the finite difference solution, system temperatures found at the nodal points used in the domain mesh. The transient energy balance for each node is written using the first law of thermodynamics. The finite difference form of the conduction heat flows, including storage, is shown below:

$$m * cp * \frac{dT}{dt} = \frac{a_x * k_x}{\Delta x} * (T_{x+\Delta x} + T_{x-\Delta x} - 2 * T_x) + \frac{a_y * k_y}{\Delta y} * (T_{y+\Delta y} + T_{y-\Delta y} - 2 * T_y) \quad (9)$$

The one dimensional finite difference grid used in the model is shown in fig. 2 below:

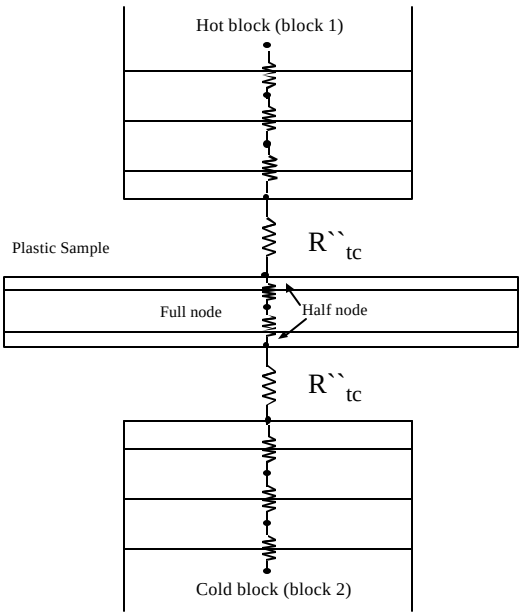

Fig 2. Finite difference grid used in data reduction.

The joint temperatures used by the lumped and distributed capacity technique differ slightly, affecting the measurements. The lumped capacitance technique defines the driving potential across the average temperature of the two blocks, whereas the distributed capacitance defines it across the slice of block in contact with the plastic. As the average temperature difference is greater than the temperature difference across the contact surfaces, for the same joint conductance the lumped capacitance solution will predict a higher heat flow between the two blocks.

When the contact resistance is being measured based on recorded temperature data, the lumped capacitance technique will predict a higher contact resistance than the distributed capacitance method. The same heat flow between the blocks is seen, and the distributed capacitance method will see a lower driving temperature potential across the interface and will then find a smaller contact resistance.

For a joint conductance measured by the distributed capacitance technique of 2000 W/m^2-K, the lumped capacitance solution would predict a 20% higher joint conductance. The distributed capacitance technique would still over predict the actual joint conductance, but by a much smaller amount. For this reason, the joint conductance of the relatively thin polyester and polypropylene plastics was calculated using the distributed capacitance analysis.

The losses to the ambient were considered by a constant heat loss parameter in the development of the finite difference equations. This proved more accurate than modeling the conduction losses through the insulation as well because the loss parameter could be fit with the experimental data.

In order to determine the contact conductance, measured temperature – time response data is compared with the response predicted by the lumped thermal capacitance approximation. The error between the measured block temperatures and the predicted temperatures was calculated at each time step. The total error for the run was then calculated as:

$$Error = \sum_{i=1}^{i=j} \sqrt{(T^{i}{}_{hp} - T^{i}{}_{hm})^2 + (T^{i}{}_{cp} - T^{i}{}_{cm})^2} \tag{9}$$

Where h, c, p and m stand for hot, cold, predicted and measured respectively. *i* was the value at each time step, and *j* was the final time step. A least squares approach was used in order to minimize the sum of the absolute value of the error at each time step.

An optimization program written in EES (5) was used to solve for the values of the parameters that yielded the 'best fit' of the analytical solution to the measured temperatures for each run. The error between the analytical solution and the measured values was minimized by varying the contact resistance, the initial temperatures of the two blocks and the loss coefficient of the blocks.

The value of the error had no intrinsic meaning, and was only a qualitative measure of how well the analytical solution fit the measured data. Smaller errors were better, but were not related to the experimental error in the contact resistance value. One hundred sample points, spaced at two second intervals, were used in each optimization run. Two hundred seconds of data was sufficient to show the exponential effect of the transient response and the losses to the ambient sink. Figure 2 below shows both the measured and predicted hot and cold block temperatures during a test.

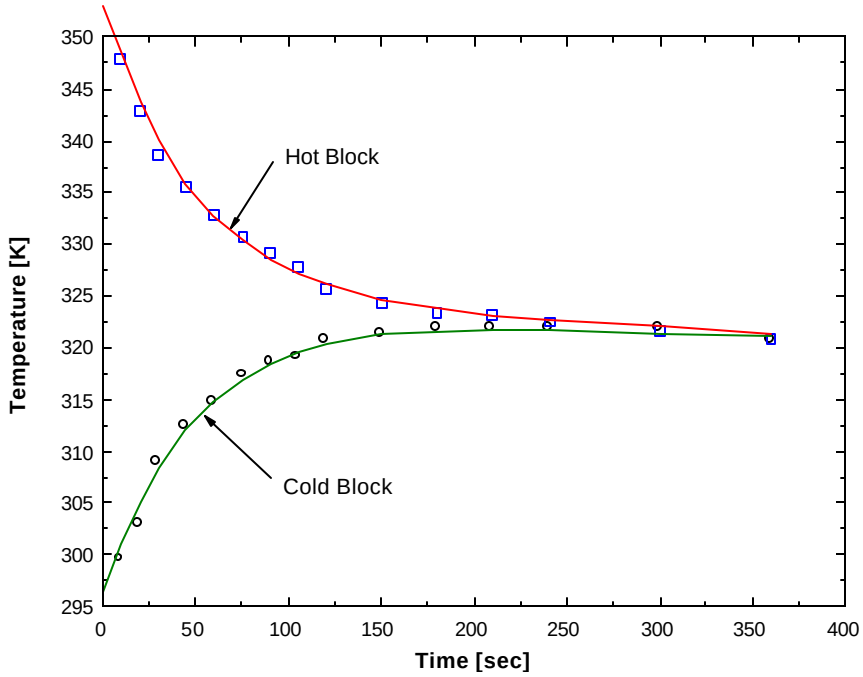

Figure 2. Predicted and experimental block temperature response.

Guess values and variable bounds were provided to the EES optimization routines. The guess values for temperature were taken from the measured temperature of the blocks, and the guess values for the loss coefficients and the contact resistance were extracted from the final results of the last run. The error for each run was quite sensitive to the varied parameters, and if the bounds of any parameters were unduly restricted a high error would result. A visual check of a plot of the best-predicted response and the actual measured temperature response of the two blocks was a good indicator of both whether the optimization had found the true minimum and how sensitive the reduction technique was to each parameter.

Representative data was used to examine the effect of sampling periods on the determined contact resistance. Both the number of samples used in the data reduction and the initial time of the samples after the blocks were placed in contact were varied. Any systematic variation in the determined contact resistance would be due to an error in the data reduction method. Plots of the joint conductance determined are shown in figure 2.5.2 and 2.5.3 below. The time of reduction is shown on the x-axis, and the joint conductance is shown on the y-axis.

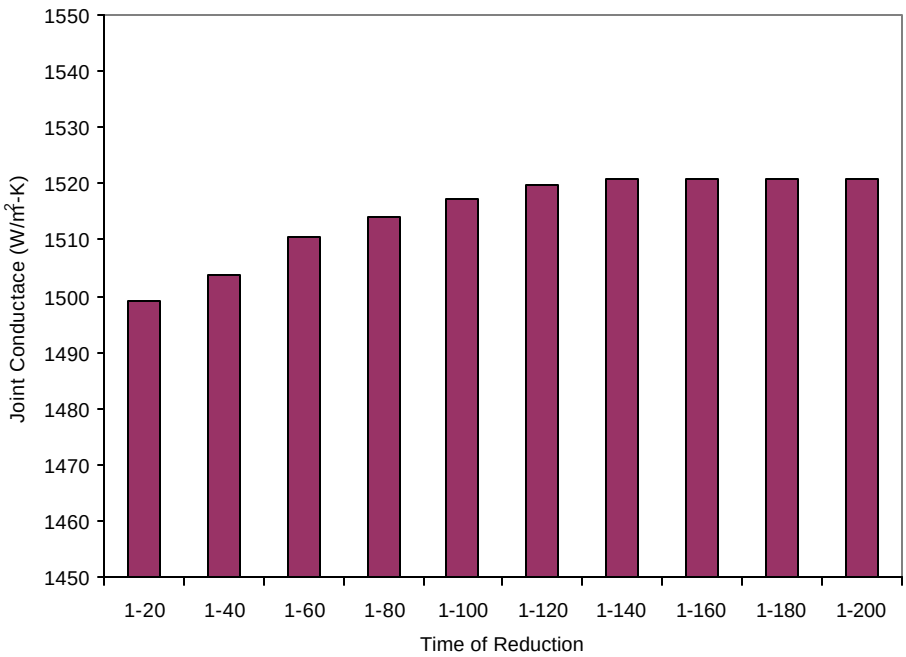

Figure 3. Determined joint conductance vs. sample time.

The conductance values are smaller for small sample periods than they are for longer data runs, and reach an asymptote at approximately 100 seconds. This is due to the initial transient response of the conduction heat flows internal to each block. The heat flows internal to the block set up an internal temperature profile based on Fouriers' law of conduction. The time constant of the temperature profile development is quicker than the time constant of the overall transient response of the hot and cold blocks together. All tests use at least 200 seconds of temperature data to ensure that the initial transients within each block are over. Additionally allowing the optimization routine to vary the initial temperatures reduced the effect of the initial transients.

If only twenty seconds worth of samples (10 actual samples) are used, but taken from different time periods in the measured response, there is a small variation in the measured contact resistance. The small variation is much less than the variation between tests for any of the samples and is probably due to thermocouple errors. Figure 4 shows the variation as a function of when the samples were taken in the test.

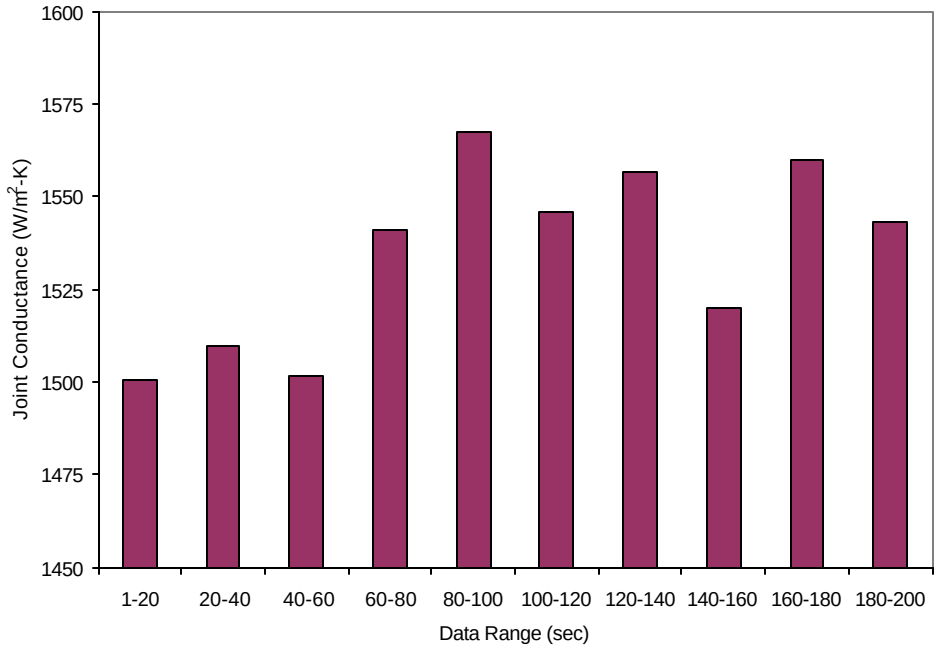

Figure 4. Determined joint conductance vs. time after initial contact.

There is no pattern in the variation of the joint conductance based on the different sample times, and the standard deviation for the series is less than 2% of the measured contact resistance. For the data taken from the start of the test, the temperatures of the blocks would still be changing rapidly, after 100 seconds however the blocks temperature would be changing more slowly. The change in temperature at the start would be much greater than the noise in the measurements, at the end of the measurement period the signal to noise ratio would be lower.

Error Analysis

The energy lost through the insulation from both blocks varied from 3 to 20 % of the total energy transferred from the top block to the bottom block. The low energy losses were for the thin polypropylene samples where the hot and cold blocks equalized quickly. The higher losses occurred with the relatively thick embossed polyethylene where the high resistance between the blocks gave more time for them to leak heat to the ambient. In both cases this energy loss is accounted for by including the loss parameter in developing the differential equations.

As the total thermal resistance between the two blocks includes the conduction resistance in the plastic, any uncertainty in the plastic properties of thickness or thermal conductivity affect the measured contact resistance in a linear fashion. While the thickness of the plastics can be accurately measured, the thermal conductivity was not constant, or accurately known, over the range of temperatures experienced in the study. The conductivity of the embossed polyethylene varied the most in this study. The conductivity varied from 0.38 to 0.25 W/m-K

under the temperature ranges found in the experiments. As the conduction resistance was 20% of the total resistance measured in the system, the maximum error due to property variation for the embossed polyethylene samples was 7%. For the polypropylene and polyester samples the error was less than 2%.

The largest source of random error was due to the flatness of the blocks. When the blocks were brought together for each test they were brought together in different orientations around the vertical axis. The flatness error of the blocks would have varying effect on the measurements of the joint resistance, but it is difficult to quantify. Due to the vastly different technique between polishing a flat surface and grinding a cylindrical roll, there were different macroscopic surface finish characteristics. The surface roughness parameter, a measure of the microscopic irregularities, can be matched, but the flatness of the blocks has no counterpart on a roller nor does the runout on the roller have a counterpart on the flat blocks.

RESULTS AND DISCUSSION

Table 1. Plastic properties and measured joint conductance measured using static tests.

		Polyester	Polypropylene	Embossed Polyethylene
Thickness	mm	0.127	0.020	0.076
ρ	kg/m^3	1004	905	920
cp	J/kg-K	1930	1340	2300
k	W/m-K	0.15	0.24	0.33
Min. $h^2_{contact}$	W/m^2-K	667	769	270
Max. $h^2_{contact}$	W/m^2-K	2000	2000	435
Avg. $h^2_{contact}$	W/m^2-K	1428	1250	345
S.D.	%	21.2	22.8	10.4

The polyester and polypropylene tested in this study have a smooth finish, and were produced by drawing a relatively thick web of plastic through nips and successively stretching the plastic to its final thickness. Plastic properties were take from (6). As the contact resistance is based primarily on the finish properties of the surfaces, the internal molecular structure of the plastics has only a small effect on the joint resistance. The plastic molecular structure will effect the thermal conduction resistance in the plastic however.

While the error in the measurements is large, it is generally better than most joint conductance measurements for low pressure loading. Other authors have commented on lack of repeatability in their measurements below 386 kpa (2).

The joint conductance data measured for the polyester and polypropylene to aluminum surface is statistically identical. Under the range of pressures used in the study, the pressure had only a small effect on the contact resistance, with slightly higher measured contact resistance at the lowest interface pressures. For the smooth plastics, the standard deviation of the 8 tests run at each pressure decreased with increasing pressure. This is

probably due to a better ‘fit’ of the sample in the test apparatus, reducing the random effect of how the plastic sample was placed between the two blocks.

Fig. 3 shows the measured joint resistance of the polyester- aluminum interface over the range of pressures used in the tests.

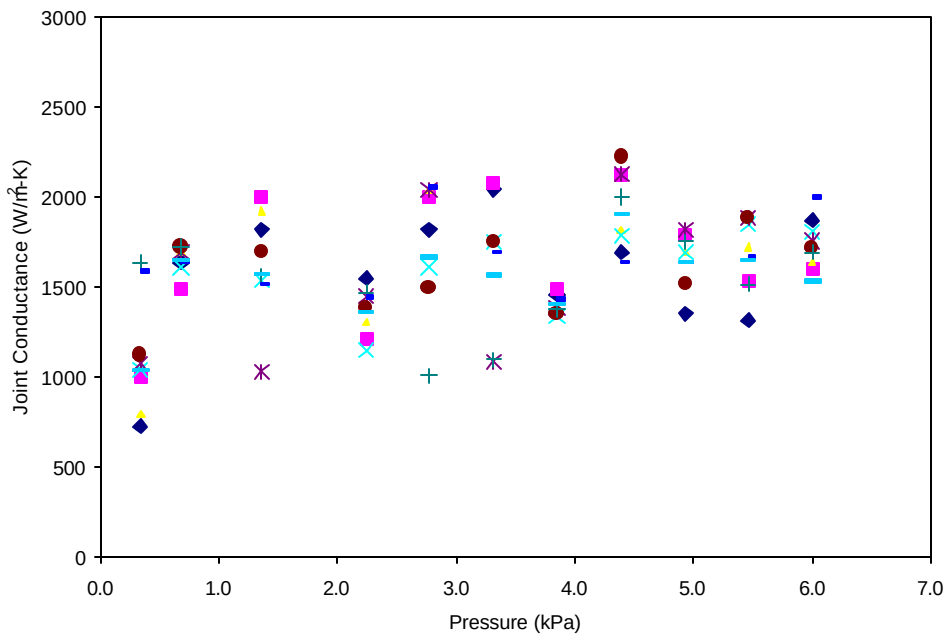

Fig. 3. Thermal joint conductance as a function of pressure for the polyester – aluminum interface

Fig. 4 shows the measured joint resistance of the polypropylene-aluminum interface over the range of pressures used in the tests.

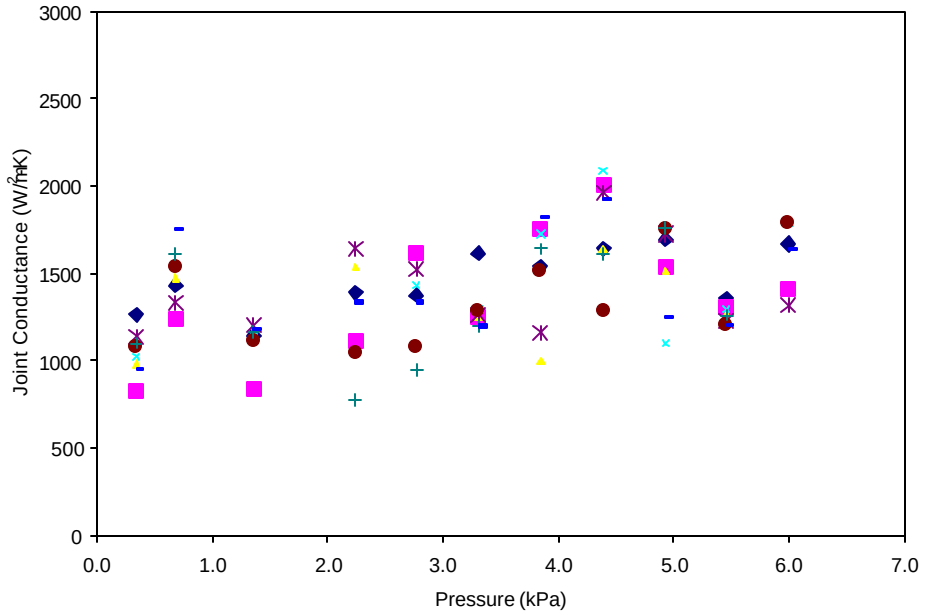

Fig. 4. Thermal joint conductance as a function of pressure for the polypropylene – aluminum interface.

The embossed polyethylene measurements showed a significantly lower joint conductance due to the roughness imposed on the plastic sheet by the embossing roller.

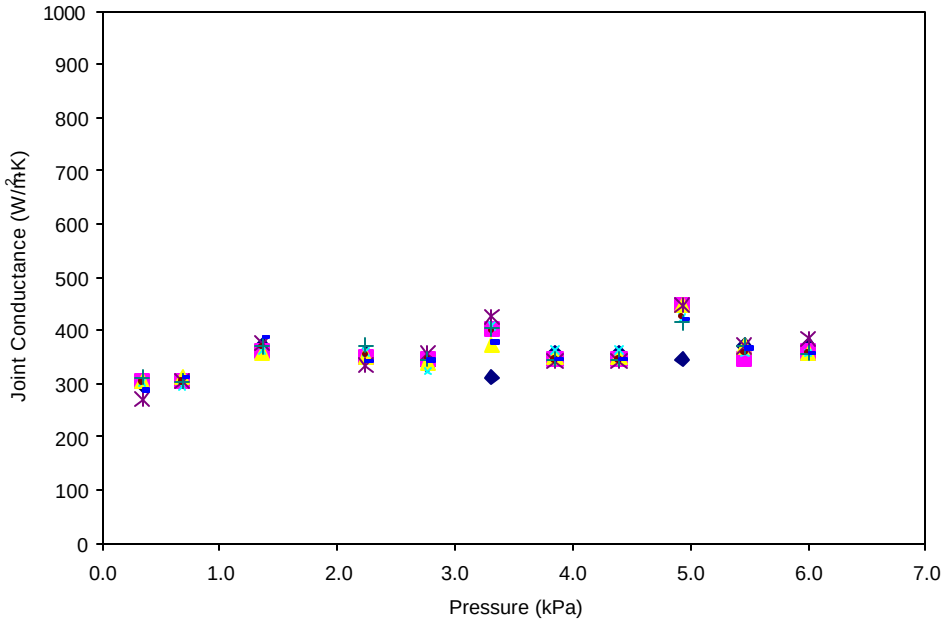

Fig. 5. Thermal joint conductance as a function of pressure for the embossed polyethylene – aluminum interface.

Any comparison with published data is hard to make due to the lack of appropriate plastic data for the pressure ranges encountered in this study. A comparison between calendered paper and the plastics can be made. Calendered paper has been densified and has a smooth surface finish similar to the smooth plastics in this study. Calendered paper was reported to have a joint conductance of 1667 W/m^2-K by Kerekes (1980), in an unnipped roller case. Similar results to Kerekes were reported by Burnside & Crotogino, (1984), again for calendered paper.

Acknowledgements

Ron Buono, American Roller Company.

References

1. Kerekes, R.J., "A simple method for determining the thermal conductivity and contact resistance of paper," Technical Association of Pulp and Paper Industries Journal, Vol. 63,
2. Sanders, D.J. Forsyth, R.C., "Measurement of Thermal Conductivity and Contact Resistance of Paper and Thin-film Materials.", Review of Scientific Instrumentation, Vol. 54, No. 2, Febuary 1983.
3. Seyed-Yagoobi, J, Ng, K.H., Fletcher L.S., "Thermal Contact Conductance of a Bone Dry Paper Handsheet/Metal Interface", ASME journal of Heat Transfer, Vol. 114, pp. 326-330, 1992a
4. Beckman,W.A., Mitchell, J., "A Technique for the Evaluation of the Thermal Conductivity of Coating Materials", Thermal Conductivity, 887 – 894, 1968.
No.9, pp. 127-140, 1980.
5. Klein, S.A., Alvarado, F.L., EES – Engineering Equation Solver, F-Chart Software, Middleton, WI, 1998.
6. Osswald, T.A., Menges, G., Materials Science of Polymers for Engineers, Hanser/Gardner, New York, 1996.

Seyed-Yagoobi, J, Ng, K.H., Fletcher L.S., "Thermal Contact Conductance of a Bone Dry Paper Handsheet /Metal Interface", ASME journal of Heat Transfer, Vol. 114, pp. 326-330, 1992a.
Roisum, D.R., The Mechanics of Rollers, Technical Association of Pulp and Paper Industries, Georgia, 1996.

1	Top (Hot) Block	6	Load Insulation
2	Bottom (Cold) Block	7	Load (Variable)
3	Plastic Sample	8	Top Thermocouple
4	Bottom Insulation Cavity	9	Bottom Thermocouple
5	Top Insulation Cavity		